Key Engineering Materials
ISSN: 1662-9795, Vol. 1049, pp 123-129
doi:10.4028/p-dyN4E6

Submitted: 2026-01-19
Accepted: 2026-02-10
Online: 2026-04-15

Application of Reference-Free Strain Measurement to Assess the Deformation Level of Pre-Deformed Components

ROSSI Marco[a]*, TANONI Giulia[b], ANEDDA Matteo[c], FIORETTI Maria Caterina[d], and PRINCIPI Emanuele[e]

Università Politecnica delle Marche, via brecce bianche 12, 60131 Ancona, ITALY

[a]m.rossi@univpm.it, [b]g.tanoni@univpm.it,[c]m.anedda@pm.univpm.it,[d]m.c.fioretti@pm.univpm.it, [e]e.principi@univpm.it

Keywords: Remanufacturing, Plastic Deformation, Convolutional Neural Network

Abstract. In the framework of sustainable manufacturing and circular economy, the reuse of metallic components at the end of their first life (EoL) is a promising strategy to reduce energy consumption and material waste, but it requires an accurate assessment of residual plastic deformation, which strongly affects structural integrity and remaining formability. Conventional full-field techniques such as Digital Image Correlation (DIC) require a reference image of the undeformed state, which is generally unavailable for EoL components. To address this limitation, this work investigates a deep learning–based, reference-free approach for strain estimation directly from a single image of the deformed surface. The method relies on a convolutional neural network architecture derived from VGG-16, trained to regress the in-plane principal strains and their orientation from local image subsets of the surface texture using a synthetically generated dataset based on real material textures and realistic imaging conditions. The trained model is applied to high-resolution optical images of pre-deformed steel and aluminum components from regions subjected to different deformation histories, with partial validation provided by finite element simulations and conventional DIC measurements. Preliminary results show that the proposed approach can distinguish regions with different levels of plastic deformation and provide strain maps consistent with independent mechanical assessments, demonstrating its potential as a rapid, non-destructive tool for deformation mapping and classification of EoL components to support remanufacturing and reuse decisions.

Introduction

Digital Image Correlation (DIC) is a well-established optical technique for measuring displacement and strain fields on the surface of solids by comparing images of an undeformed configuration with those acquired during deformation [1]. Over the years, DIC has evolved into a versatile framework, including stereo-DIC for 3D measurements, multi-camera configurations, optical extensions of single-camera systems [2], and full 360○ strain measurements [3]. Extensions such as Digital Volume Correlation (DVC) further enable the reconstruction of three-dimensional deformation fields inside solids [4, 5]. Thanks to these capabilities, DIC has become a key tool in material characterization [6], enriching the information obtained from mechanical tests and supporting modern paradigms such as Material Testing 2.0 [7]. It is also widely used for the experimental validation of numerical models, including finite element simulations [8].

In parallel, recent advances in Deep Learning (DL) across several domains, ranging from time series analysis [9, 10] to image processing [11], have stimulated growing interest in DL-based approaches for DIC [12]. Convolutional Neural Networks (CNNs), in particular, have been investigated as alternatives or complements to traditional correlation algorithms. Previous studies proposed CNNs to directly estimate displacement and strain fields by mimicking the classical DIC workflow, showing improvements in computational efficiency and accuracy [13, 14].

In this work, we apply a different approach. Instead of replicating the image correlation process, we introduce a deep learning-based approach capable of estimating the deformation level directly and solely from the deformed image. Similar ideas have recently been explored in microfluidic applications for inferring three-dimensional information from defocused images [15, 16], but only very

recently they have been applied to deformation measurements in solid mechanics [17]. By removing the need for a reference image, the proposed approach enables deformation analysis in scenarios where classical DIC is not applicable, such as post-mortem microstructural observations where only deformed images are available. Our current implementation, termed *DeepStrainNet*, is based on the VGG-16 architecture [18]. The proposed methodology is here applied to synthethic and real deformed materials.

Methods

Conventional subset-based Digital Image Correlation (DIC) estimates the displacement field by matching subsets between undeformed and deformed images, while strain is obtained by spatial differentiation of the displacement field. In contrast, the proposed approach directly estimates the strain field from a single deformed image by means of a deep learning model trained to recognize the deformation of a known surface pattern.

A planar deformation state is described by the two principal strains, ε_1 and ε_2, and the orientation θ of the principal directions. These three continuous variables define the output of the proposed method, which is therefore formulated as a regression problem. The input of the network is a grayscale image subset $\mathbf{X} \in \mathbb{R}^{N \times M \times 1}$, while the output is the vector $\mathbf{d} = [\varepsilon_1, \varepsilon_2, \theta]^T$. The neural network implements a parametric function

$$\mathbf{d} = \mathbf{f}_{\boldsymbol{\Theta}}(\mathbf{X}), \tag{1}$$

where $\boldsymbol{\Theta}$ denotes the set of trainable parameters.

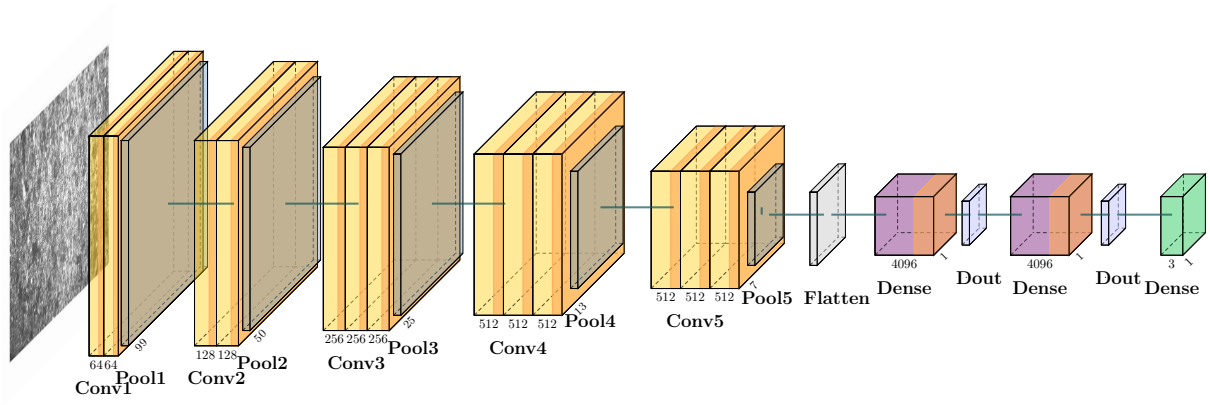

Fig. 1: The proposed neural network architecture. Differently from the standard VGG-16 architecture, the last layer has 3 outputs, one for each deformation parameter. The output can be modified if only one deformation is required.

Neural network architecture. The function $\mathbf{f}_{\boldsymbol{\Theta}}(\cdot)$ is implemented using a convolutional neural network named *DeepStrainNet*, derived from the VGG-16 architecture [18]. The convolutional backbone of VGG-16 is retained as a feature extractor, while the original classification head is replaced with a regression head composed of fully connected layers. The final output layer consists of three neurons with linear activation, corresponding to the deformation parameters ε_1, ε_2, and θ. A schematic representation of the architecture is shown in Fig. 1.

Training procedure. The network parameters are learned from a labeled dataset of image subsets and corresponding ground-truth deformation parameters. Training is performed by minimizing the Mean Squared Error (MSE) loss between predicted and target values. Optimization is carried out using the Adam optimizer, with a learning rate scheduled according to a cosine decay strategy.

Test on Simulated Microstructure

As first case study, the method is applied to reconstruct a strain localization within the microstructure. In this case, only simulated experiments are used. The images are generated through a numerical simulator capable of reproducing realistic deformation effects while accounting for typical experimental uncertainties, such as image noise and illumination variations [19]. This type of simulator is widely used in experimental mechanics to evaluate the performance and uncertainty of measurement and identification techniques [20, 21]. Synthetic images are also routinely employed for benchmarking deformation measurement methods, including DIC algorithms [22].

The image generation procedure is based on the optical flow conservation principle, whereby the gray-level distribution of an undeformed microstructural image is mapped onto a deformed configuration through a prescribed kinematic transformation [23]. Starting from a high-resolution reference micrograph, treated as a continuous gray-level field via cubic interpolation, deformed images are obtained by applying analytical displacement fields corresponding to homogeneous planar deformation states.

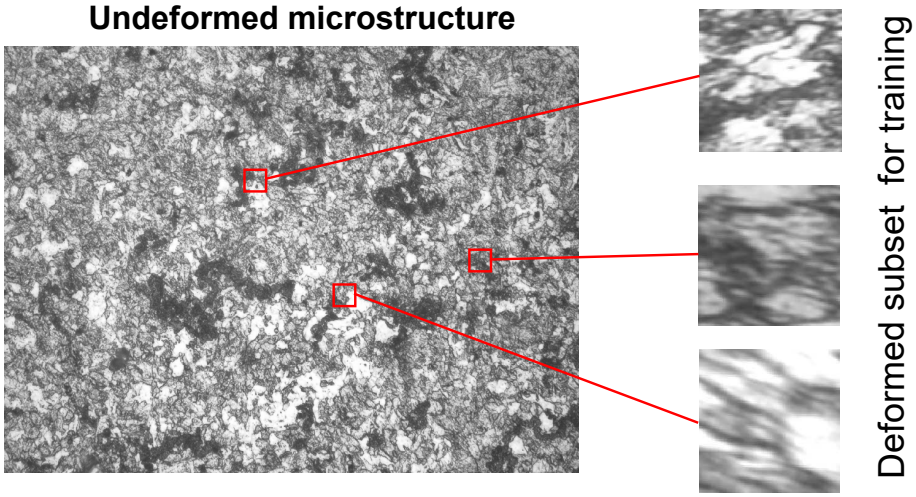

Fig. 2: Generation of the images for the training set: deformed subset of 99×99 pixel are generated randomly starting from a given undeformed microstructure.

The training set is obtained using the DT to generate a series of N deformed images (size of 99×99 pixels) with constant principal strains ε_1 and ε_2 and an in-plane rotation angle θ. The strain parameters are randomly sampled within predefined ranges corresponding to tensile and shear dominated deformation regimes [17], see Fig. 2. To enhance realism, experimental uncertainties are introduced through the DT, including additive gray-level noise and spatially varying illumination changes. This procedure enables the generation of a large number of statistically independent deformed microstructural images starting from a limited set of reference micrographs, by jointly varying the deformation level and the local microstructural features. In this study, the synthetic dataset is generated exclusively from optical micrographs of an X65 steel microstructure. A series of $25\,000$ images were genereated and used to train the Convolutional Neural Network.

The trained network was used to retrieve the deformation in a newly generated microstructure, subjected to a deformation field prescribed according to a sinusoidal function, leading to the formation of periodic strain localization bands. The maximum value of the principal strain component ε_1 was set to 0.5. Differently from the training set, the deformation was applied to the entire reference image through a spatially non-uniform mapping, rather than by assigning a constant strain field to a 99×99 sub-image. This procedure allows for the generation of continuously varying deformation gradients and enables a direct assessment of the method capability to capture deformation gradients and strain heterogeneities.

The deformed image was obtained starting from a micrograph of the same material used in the training phase, but extracted from a different specimen region and therefore not included in the training dataset. This choice ensures that the evaluation is performed on previously unseen microstructural features, thus providing a meaningful validation of the generalization capability of the network.

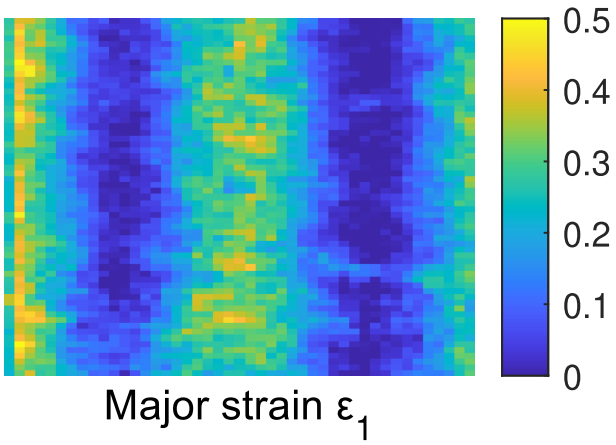

Fig. 3: Deformation field of the deformed microstructure obtained with the trained CNN. The principal strain is shown, the localization bands are clearly visible.

Fig. 3 reports the deformation strain field reconstructed by the proposed algorithm. The results show that the method is able to properly capture both the amplitude and the spatial distribution of the strain localization bands, demonstrating its effectiveness in reproducing the underlying deformation pattern.

Experimental Validation on an Aluminum Sample

A further validation of the proposed methodology was carried out on real experimental data acquired during a uniaxial tensile test. The investigated material is an aluminum alloy AA5754, commonly used in forming applications due to its good combination of strength and ductility.

The displacement and strain fields were measured by means of a commercial Digital Image Correlation (DIC) software, namely MatchID, which was employed to provide a reference strain field for comparison with the results obtained by the proposed method. The obtained principal strain field is illustrated in Fig. 4.

On the opposite face of the specimen, where no speckle pattern was applied, the surface was observed by means of an optical microscope at $200\times$ magnification. An angular illumination was adopted in order to enhance the surface roughness features. A different surface behavior is observed at low and high deformation levels, as shown in Fig. 4. At low strain, the surface appears more regular with clear linear features, that tends to reduce a higher strain levels.

A series of random sub-images of size 99×99 pixels were extracted from the microscope images acquired over the whole specimen surface. These patches were used to build the dataset for training and validation of the network. A subset of such images was employed for training, while the remaining ones were reserved for testing. In this case, only one strain component was considered for training, namely the principal strain. A total of $20\,000$ images were used for training the network, whereas $4\,500$ images were selected as a test set. Importantly, the test images were extracted from a different region of the specimen with respect to the training set, so as to ensure a strict spatial separation between training and validation data and to avoid any bias due to local correlations.

Fig. 5 shows the results obtained on the test set compared with the DIC reference. A good agreement between the predicted and reference strain values is observed, thus confirming the ability of the proposed approach to generalize to previously unseen regions of the specimen.

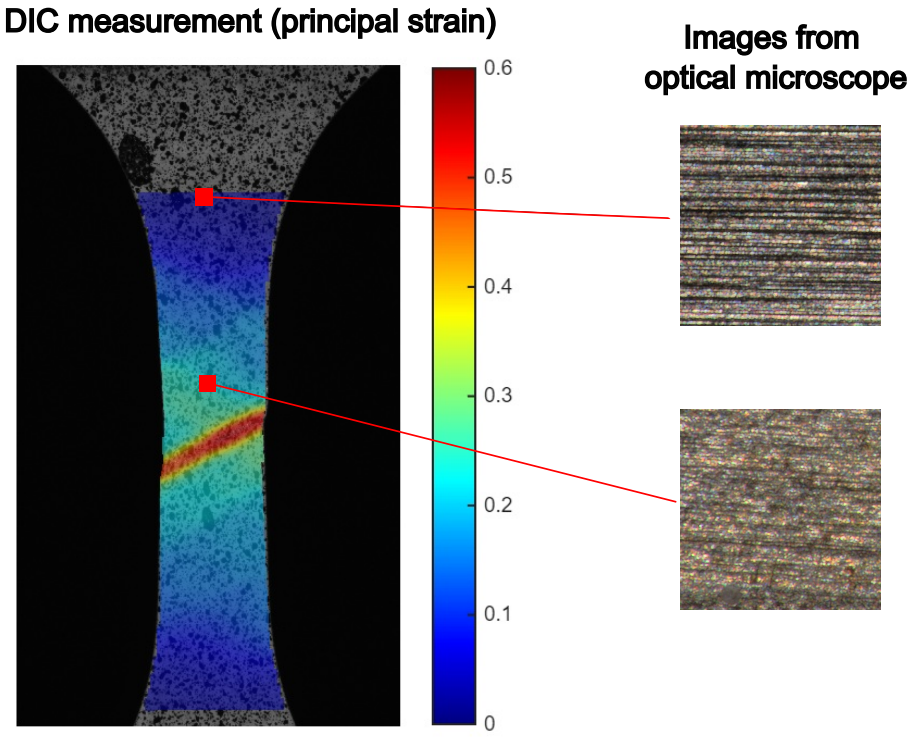

Fig. 4: Deformation map obtained with DIC and examples of the surface roughness observed with the optical microscope.

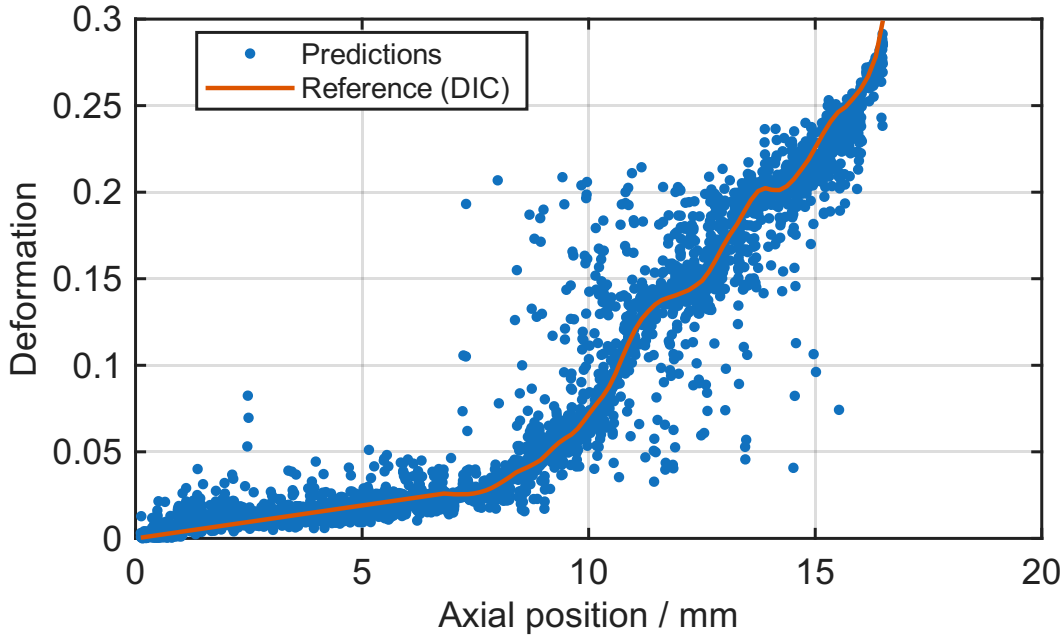

Fig. 5: Comparison of the predictions obtained with the trained CNN with respect to the reference DIC measurement; the major principal deformation is considered.

Conclusions

In this work, a deep learning–based, reference-free approach for full-field strain estimation from a single deformed image has been presented and validated on both synthetic and experimental data. Differently from conventional Digital Image Correlation techniques, the proposed method does not require access to an undeformed reference configuration, thus enabling deformation assessment in scenarios where classical approaches are not applicable, such as post-mortem analyses or remanufacturing applications.

The method was first validated on synthetically generated microstructural images, where complex and spatially varying strain fields were successfully reconstructed, including strain localization bands induced by non-uniform deformation gradients. Subsequently, the approach was applied to real experimental data acquired during a tensile test on an AA5754 aluminum alloy specimen, showing good agreement with independent DIC measurements.

A key outcome of this study is that the proposed methodology proved to be effective independently of the nature of the surface pattern used as input. In particular, reliable strain estimations were obtained both from intrinsic material microstructures and from surface roughness features observed by optical microscopy, without the need for an artificial speckle pattern.

These results highlight the versatility and robustness of the proposed approach and open the way to its application in a wide range of practical scenarios, including the inspection and classification of end-of-life components for remanufacturing, where surface conditions and textures may vary significantly from case to case.

Future work will focus on extending the method to multiaxial loading conditions, improving quantitative accuracy through larger experimental datasets, and exploring its integration into industrial inspection pipelines.

Acknowledgement

This work was carried out within the framework of the project “Going Beyond Recycling: Reshaping of End-of-Life Components through Advanced Sheet Metal Forming Processes”, funded under the PRIN 2022 Call (MUR Decree No. 1401 of 18/09/2024 - CUP I53C24002500006).

References

[1] M.A. Sutton, J.J. Orteu and H. Schreier: Springer, Image Correlation for Shape, Motion and Deformation Measurements (2009).

[2] K. Genovese, L. Casaletto, J.A. Rayas, V. Flores and A. Martinez: Optics and Lasers in Engineering Vol. 51 (2013), p. 278.

[3] K. Genovese, L. Cortese, M. Rossi and D. Amodio: Optics and Lasers in Engineering Vol. 82 (2016), p. 127.

[4] B. Pan and B. Wang: Optics and Lasers in Engineering Vol. 135 (2020), p. 106189.

[5] M. Rossi, L. Cortese, K. Genovese, A. Lattanzi, F. Nalli and F. Pierron: Experimental Mechanics Vol. 58 (2018), p. 1181.

[6] S. Avril, M. Bonnet, A.-S. Bretelle, M. Grédiac, F. Hild, P. Ienny, F. Latourte, D. Lemosse, S. Pagano and E. Pagnacco: Experimental Mechanics Vol. 48 (2008), p. 381.

[7] F. Pierron and M. Grédiac: Strain Vol. 57 (2021), p. e12370.

[8] P. Lava, E.M.C. Jones, L. Wittevrongel and F. Pierron: Strain Vol. 56 (2020), p. e12350.

[9] G. Tanoni, E. Principi, L. Mandolini and S. Squartini: in Applied Intelligence and Informatics, Springer (2022), p. 360.

[10] G. Tanoni, L. Stankovic, V. Stankovic, S. Squartini and E. Principi: IEEE Trans. Ind. Informatics Vol. 20 (2024), p. 4710.

[11] M. Trigka and E. Dritsas: Sensors Vol. 25 (2025).

[12] X. Duan, H. Xu, R. Dong, F. Lin and J. Huang: Optics and Lasers in Engineering Vol. 160 (2023), p. 107234.

[13] Y. Wang and C. Zhou: Optics and Lasers in Engineering Vol. 174 (2024), p. 107981.

[14] Y. Feng and L. Wang: Optics and Lasers in Engineering Vol. 179 (2024), p. 108267.

[15] R. Barnkob, C. Cierpka, M. Chen, S. Sachs, P. Mäder and M. Rossi: Measurement Science and Technology Vol. 32 (2021), p. 094011.

[16] M. Mehdizadeh Youshanlouei and M. Rossi: Physics of Fluids Vol. 36 (2024).

[17] M. Rossi, G. Tanoni, V. Ilari, M. Sasso and E. Principi: Submitted to Engineering Application of Artificial Engineering, SSRN preprint (2025).

[18] K. Simonyan and A. Zisserman: Proc. ICLR (2015).

[19] M. Rossi, P. Lava, F. Pierron, D. Debruyne and M. Sasso: Strain Vol. 51 (2015), p. 206.

[20] M. Badaloni, M. Rossi, G. Chiappini, P. Lava and D. Debruyne: Experimental Mechanics Vol. 55 (2015), p. 1411.

[21] A. Peshave, F. Pierron, P. Lava, D. Moens and D. Vandepitte: Strain Vol. 60 (2024), p. e12473.

[22] P.L. Reu, E. Toussaint, E. Jones, H.A. Bruck, M. Iadicola, R. Balcaen, D.Z. Turner, T. Siebert, P. Lava and MDIC Simonsen: Experimental Mechanics Vol. 58 (2018), p. 1067.

[23] M. Rossi and F. Pierron: Int. J. Solids Struct. Vol. 49 (2012), p. 420.